

PAPER • OPEN ACCESS

# Real-time control of a hearing instrument with EEG-based attention decoding

To cite this article: Jens Hjortkjær *et al* 2025 *J. Neural Eng.* **22** 016027

View the [article online](#) for updates and enhancements.

## You may also like

- [Real-time TMS-EEG for brain state-controlled research and precision treatment: a narrative review and guide](#)  
Miles Wischniewski, Sina Shirinpour, Ivan Alekseichuk et al.
- [Geometric neural network based on phase space for BCI-EEG decoding](#)  
Igor Carrara, Bruno Aristimunha, Marie-Constance Corsi et al.
- [Neural decoding and feature selection methods for closed-loop control of avoidance behavior](#)  
Jinhan Liu, Rebecca Younk, Lauren M Drahos et al.



## PAPER

## OPEN ACCESS

RECEIVED  
29 February 2024

REVISED  
8 July 2024

ACCEPTED FOR PUBLICATION  
14 October 2024

PUBLISHED  
25 February 2025

Original Content from  
this work may be used  
under the terms of the  
[Creative Commons  
Attribution 4.0 licence](#).

Any further distribution  
of this work must  
maintain attribution to  
the author(s) and the title  
of the work, journal  
citation and DOI.



# Real-time control of a hearing instrument with EEG-based attention decoding

Jens Hjortkjær<sup>1,2,\*</sup> , Daniel D E Wong<sup>3,4</sup> , Alessandro Catania<sup>1</sup> , Jonatan Märcher-Rørsted<sup>1</sup>, Enea Ceolini<sup>5</sup> , Søren A Fuglsang<sup>1,2</sup> , Ilya Kiselev<sup>5</sup> , Giovanni Di Liberto<sup>6</sup> , Shih-Chii Liu<sup>5</sup> , Torsten Dau<sup>1</sup> , Malcolm Slaney<sup>7</sup> and Alain de Cheveigné<sup>3,4</sup>

<sup>1</sup> Hearing Systems Section, Department of Health Technology, Technical University of Denmark, Kgs. Lyngby, Denmark

<sup>2</sup> Danish Research Centre for Magnetic Resonance, Centre for Functional and Diagnostic Imaging and Research, Copenhagen University Hospital—Amager and Hvidovre, Copenhagen, Denmark

<sup>3</sup> Laboratoire des Systèmes Perceptifs, CNRS UMR, Paris 8248, France

<sup>4</sup> Département d'Etudes Cognitives, Ecole Normale Supérieure, PSL, Paris, France

<sup>5</sup> Institute of Neuroinformatics, University of Zurich and ETH Zurich, Zurich, Switzerland

<sup>6</sup> School of Computer Science and Statistics, Institute of Neuroscience, Trinity College, The University of Dublin, Dublin, Ireland

<sup>7</sup> Center for Computer Research in Music and Acoustics (CCRMA), Stanford University, Stanford, CA, United States of America

\* Author to whom any correspondence should be addressed.

E-mail: [jhjort@dtu.dk](mailto:jhjort@dtu.dk)

**Keywords:** EEG, attention decoding, BCI, hearing

## Abstract

Enhancing speech perception in everyday noisy acoustic environments remains an outstanding challenge for hearing aids. Speech separation technology is improving rapidly, but hearing devices cannot fully exploit this advance without knowing which sound sources the user wants to hear. Even with high-quality source separation, the hearing aid must know which speech streams to enhance and which to suppress. Advances in EEG-based decoding of auditory attention raise the potential of neurosteering, in which a hearing instrument selectively enhances the sound sources that a hearing-impaired listener is focusing their attention on. Here, we present and discuss a real-time brain–computer interface system that combines a stimulus–response model based on canonical correlation analysis for real-time EEG attention decoding, coupled with a multi-microphone hardware platform enabling low-latency real-time speech separation through spatial beamforming. We provide an overview of the system and its various components, discuss prospects and limitations of the technology, and illustrate its application with case studies of listeners steering acoustic feedback of competing speech streams via real-time attention decoding. A software implementation code of the system is publicly available for further research and explorations.

## 1. Introduction

Listeners with normal hearing can follow speech in ‘cocktail party’ scenarios with competing speech sources by selectively attending to relevant speakers (Cherry 1953, Yost 1997). Hearing loss greatly reduces this ability, even when the sound input to the ear is amplified by a hearing aid (Bronkhorst 2000). Consequently, difficulties with communication in everyday noisy situations continue to be the most common complaint from hearing-aid users (Kochkin 2010, Lesica 2018). Acoustic amplification or noise suppression in hearing aids can restore some level

of audibility, and sound separation algorithms can suppress unwanted sounds to some degree, but the hearing aid cannot help a user follow an individual speech stream among many without knowing which stream the user wants to listen to. Even if the hearing instrument could perform high-quality acoustic scene analysis and separate all the individual sound sources in a complex acoustic environment, it still needs to know which sound sources to enhance and which to suppress. This requires a user input to the hearing aid.

Consequently, the idea of a *cognitively controlled hearing aid* has been proposed to overcome this basic

challenge (cocoha.org, Dau *et al* 2018, Slaney *et al* 2020, Geirnaert *et al* 2021). If a user's selective auditory attention can be measured from brain signals, then the brain-decoded attention signal can be used to control a speech separation process within the hearing instrument. The attention signal would then be used to control the relative levels of competing speakers in real time. Such a hearing instrument would constitute a form of neural prosthesis that assists the hearing-impaired listener by automatically enhancing relevant sound sources in a complex acoustic scene.

The vision of this neuro-steered hearing technology has been fueled by successes in auditory attention decoding from EEG or other neurophysiological signals (Mirkovic *et al* 2015, O'Sullivan *et al* 2015, Akram *et al* 2016, Aroudi *et al* 2016, Van Eyndhoven *et al* 2016, Miran *et al* 2018, Ciccarelli *et al* 2019). In offline attention decoding studies, a main direction has been to examine the correlation between continuous EEG responses to speech mixtures and acoustic stimulus features of competing speech streams (Ding and Simon 2012a, O'Sullivan *et al* 2015). The main observation is that low-frequency cortical activity ( $<10$  Hz) synchronizes with slow fluctuations in the speech envelope ( $<10$  Hz) and that this synchronization is stronger for attended speech streams compared to ignored ones (Mesgarani and Chang 2012, Power *et al* 2012, Ding and Simon 2012b, Golumbic *et al* 2013). In seminal work, O'Sullivan *et al* (2015) used a linear regression model to reconstruct speech envelopes from continuous multi-channel EEG responses to natural speech. When selectively attending to one speaker in a two-talker mixture, the speech envelopes reconstructed from the EEG responses were more correlated with the envelope of the attended speech stream compared to the ignored one. This, in turn, allowed listeners' attention to be predicted from single-trial (1 min) EEG data (O'Sullivan *et al* 2015). Later studies have demonstrated that EEG-based attention decoding with similar models can also be achieved in more realistic acoustic scenarios (Fuglsang *et al* 2017, Aroudi *et al* 2019), with shorter EEG data segments (Ciccarelli *et al* 2019, de Cheveigné *et al* 2021, Thakkar *et al* 2024), and in older listeners with hearing loss (Fuglsang *et al* 2020).

These successes obtained in an offline setting with sustained attention tasks raise hope for a real-time implementation where the brain-decoded signal steers the acoustic feedback to the listener to facilitate comprehension (e.g. in a hearing aid). In a real-time system, EEG decoding is coupled with an acoustic speech separation system that separates different voices in the listening space. The decoded attention signal controls the relative gains of the separated channels, enhancing attended sources and suppressing interfering ones. The change in the relative level

of the speech sources influences the neural response (Ding and Simon 2012a, Das *et al* 2018), creating a closed feedback loop (see figure 1). This closed loop, of which the user is a part, immediately raises several challenges. For instance, if an ignored speech stream has been attenuated by the brain-computer interface (BCI), can the user then switch attention to that stream? Is there a minimum amplitude below which this is no longer possible? Does visual feedback affect this situation, for example by helping to decode a stream when its audibility is low? How tolerant are users to inevitable processing latency and errors? How accurate and fast must the device be to be usable in real-life communication? How should the acoustic signal be rendered to the user (spatialization, etc)? How can the acoustic speech separation strategy be integrated within the small form factor of a hearing aid? Should the BCI seek to enhance attended sources or suppress ignored ones? Does the benefit require training, and can typically elderly hearing-impaired people adapt to the device and learn to harness its power?

Here we present a real-time implementation of such a closed-loop auditory attention decoding system. Our system addresses each requirement of a real device (hardware, software, usability) as explored within in the COCOHA project (<https://cocoha.org/>). It consists first of a wireless multi-microphone hardware platform that performs online low-latency acoustic speech separation via spatial beamforming. Next, an attention decoding module performs online analysis of the correlation between speech stimulus features of the separated speech streams and continuous EEG signals. By correlating the EEG to envelope features of each speech stream in a mixture, the decoder identifies the attended stream as the most correlated one. The decoded attention signal is then used to steer the relative gains of the separated speech streams to enhance the attended speaker in the acoustic feedback to the listener.

Real-time attention decoding was pioneered at the Telluride Neuromorphic Engineering Workshop in 2012, which inspired several of the offline studies mentioned above (O'Sullivan *et al* 2015). More recent attempts have focused on online decoding (Zink *et al* 2016, Aroudi *et al* 2021) or hardware implementation (Ha *et al* 2023). Our system, completed in 2018, presents an ambitious attempt to integrate hardware components for speech separation and brain decoding into one system (Wong *et al* 2018b). The current paper presents an overview of this work. In section 2 we describe the various components of the system in overview. Section 4 shows demonstrations of real-time gain steering of competing audio signals in listeners with hearing impairment and with visual inputs of the speakers face. Details of the implementation and the demonstrations are given in section 3.

Finally, we discuss the limitations and prospects of the cognitively controlled hearing technology in a broader context in section 5.

## 2. The real-time system in overview

### 2.1. Overview of the system

Figure 1 shows an overview of the real-time system. First, mixed sound signals in a free-field acoustic environment are picked up by a wireless microphone array placed in the listening space. A hardware platform synchronizes microphone signals between each other and performs low-latency beamforming to output separate speech streams corresponding to  $N$  different speakers in the listening space (section 2.2). Concurrently with this audio processing, EEG signals are recorded from the listener's scalp and synchronized with the audio signals. Synchronized EEG and audio signals are then streamed to an attention decoding module (section 2.3). The attention decoding module estimates which stream is currently being attended to by the listener, and this knowledge is used to modulate the relative gains of the audio channels in the mixture (section 2.4). The re-rendered audio mixture with the attended speaker enhanced is then presented to the listener via an insert earpiece (e.g. a hearing aid speaker).

### 2.2. Microphone array platform and acoustic scene analysis

Modern hearing aids are equipped with multiple microphones that allow the signal-to-noise ratio (SNR) of the sound to be improved via array processing. However, the close spacing between microphones, and distance from sources (both target and interferers) severely limits this benefit. We identified this as a serious bottleneck, and thus investigated the option of an ad hoc array of distributed microphones, communicating wirelessly. In an ad hoc array, the microphones occupy arbitrary positions, and the beamformer adapts to this geometry (in contrast to preset array geometries commonly proposed in the literature). This allows for large inter-microphone distances and potential proximity with sources.

For flexibility, we designed a microphone-equipped module capable of serving both as a remote node, and as a proximal node connected to the hearing aid (which can also function in the absence of remote nodes). This custom microphone/wireless hardware platform (called WHISPER) is described in detail in Kiselev *et al* 2017 and Ceolini *et al* 2020b. In brief, each module supports up to four microphones (see figure 2), and can be combined to form a sensor network of any arbitrary number. Microphone

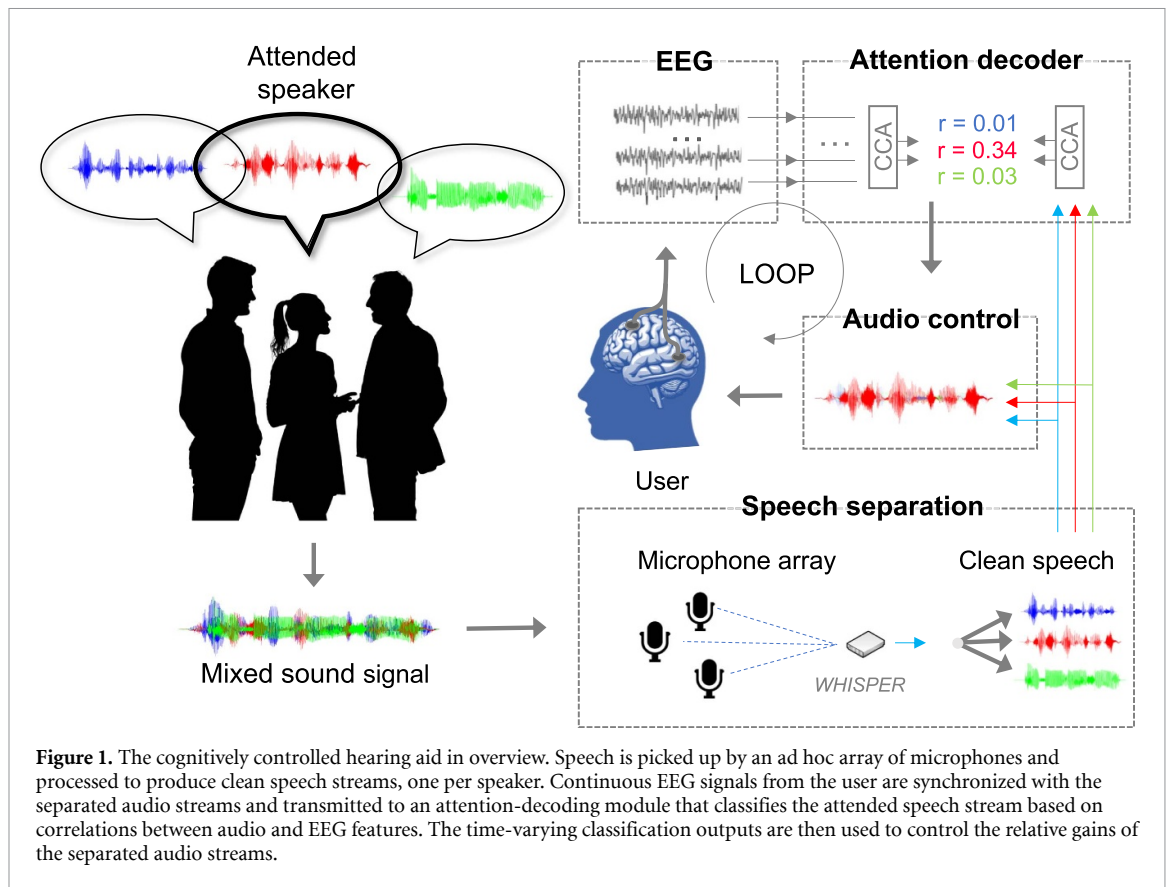
signals are synchronized wirelessly between modules, and the array can then be used for low-latency, high-quality speech separation via beamforming computed locally on the platform. Local computing capabilities allows the computational burden of potentially complex separation algorithms to be distributed.

Theory allows for infinite interferer rejection as long as the number of microphones is at least equal to the number of sources (target and interferers). However, in the presence of noise and reverberation, or for certain degenerate configurations, a larger number of microphones may provide better performance, as observed empirically. It also offers leverage to minimize spectral distortion of the target as a result of propagation and spatial filtering.

WHISPER can be used to deploy any separation or enhancement algorithm given its ability to run floating-point algebra. For our real-time BCI, we used the simple but powerful minimum-variance distortionless response (MVDR) beamforming algorithm. In evaluations of speech separation quality within a reverberant room with 2–4 speaker mixtures (with *a priori* SNR = 0), MVDR on WHISPER obtains a signal-to-distortion (SDR) of  $\sim 6$  dB using 1 WHISPER node (4 microphones), and  $\sim 9$  dB SDR using 3 nodes (12 microphones, see Ceolini *et al* 2020b). This corresponded to a short-time objective intelligibility score of 0.6 and 0.9, respectively. We have also evaluated WHISPER running other similar beamforming algorithms, such as the speech distortion weighted multichannel Wiener filter, maximum SNR, masked-based MVDR or mask-based generalized eigenvalue, with equivalent high performance (Ceolini *et al* 2020b). Notably, WHISPER can also be used to deploy high-performing speech enhancement algorithms based on deep neural networks (see Ceolini and Liu 2019).

Achieving low latency is critical for successful applications in hearing technology. Two terms contribute to latency: that of the beamformer calculation (roughly 11 ms for a 512-sample buffer with 75% overlap at 24 kHz (see Ceolini *et al* 2020b)), and that of the wireless transmission protocol. WHISPER was implemented with off-the-shelf wireless protocols, the optimization of which is a target for future work. A third, negative term applies to distant sources as a result of faster wireless than acoustic transmission.

A demonstration of our BCI shown in section 4.1 below were conducted using a single WHISPER module (with 4 microphones) wired to a remote laptop running an MVDR beamformer. In this situation, the processing latency is essentially the algorithmic latency, roughly 11 ms.

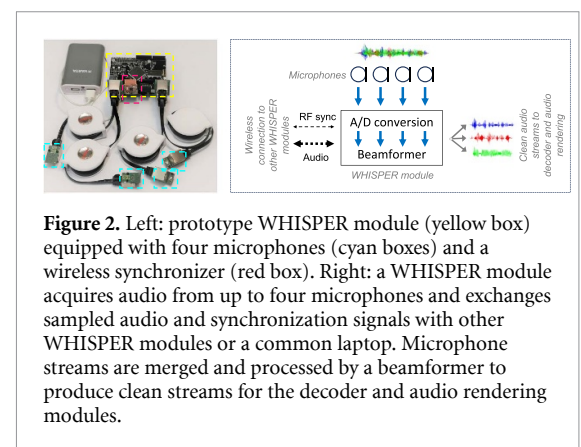


### 2.3. Attention decoding

The real-time attention decoding pipeline is illustrated in figure 3. The decoder receives the separated audio streams from the microphone platform and multichannel EEG amplifier using LabStreamingLayer (Kothe *et al* 2014). EEG and audio streams are synchronized via an initial trigger pulse sent along both paths before each experiment. The online processing pipeline, implemented in OpenVibe (Renard *et al* 2010), then performs pre-processing of both EEG and audio streams (figure 3 blue), including multichannel envelope extraction for the audio signals, and standard filtering and denoising for the EEG (see section 3 for additional details).

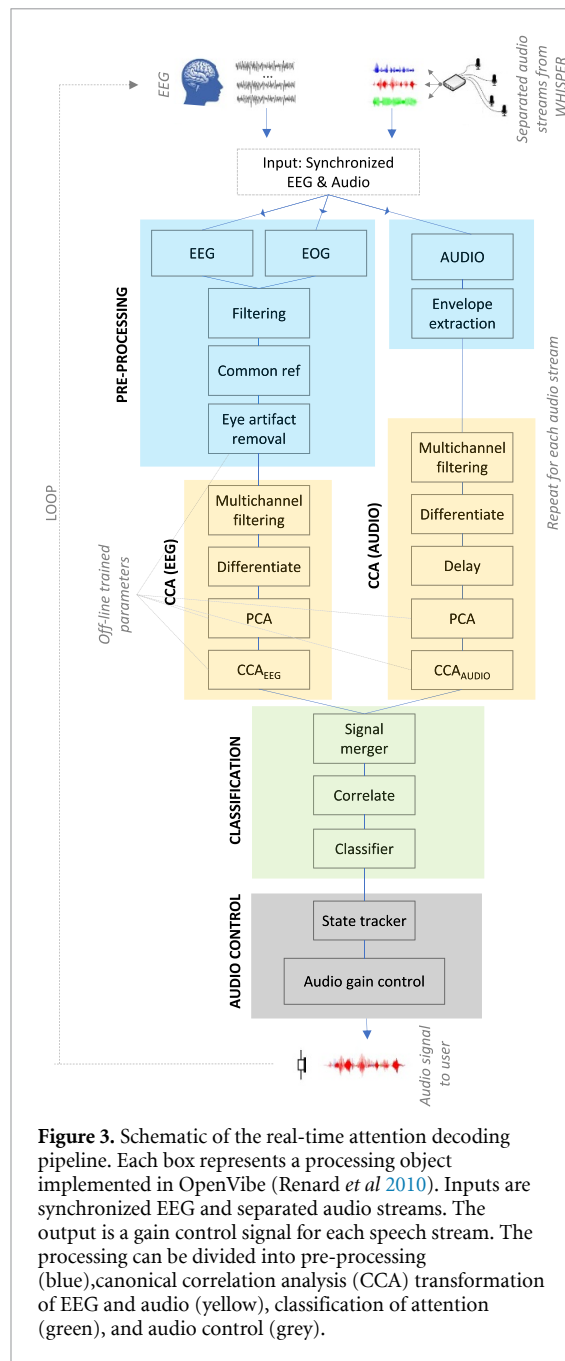
The core of the attention classification pipeline is a real-time implementation of a linear decoder based on canonical correlation analysis (CCA) (see de Cheveigné *et al* 2018 for additional details). This approach generalizes linear regression models to predict synchronized stimulus-response activity (de Cheveigné *et al* 2018, 2021). The appeal of CCA over previous forward (prediction) and backward (reconstruction) regression methods is greater accuracy (de Cheveigné *et al* 2018).

Based on training data, a CCA model is trained to find linear transforms that are then applied to both EEG and audio features from each audio stream at test time (figure 3, yellow). As inputs to the CCA model, the EEG and audio streams are passed through a



multichannel filterbank that allows the CCA solution to implement filters that equalize the spectral content of both streams, and help factor out irrelevant components at multiple time scales. The filterbanks are identical on the EEG and audio side. On the EEG side, the CCA solution implements a spatiotemporal filter to capture different neural sources correlated with stimulus activity (de Cheveigné *et al* 2018). On the audio side, the CCA combines envelope subbands to perform bandpass filtering that capture envelope fluctuations at different time scales (Dau *et al* 1997). Once the CCA weight matrices are learned on training data, the linear transformation of the data simply consists of parallel matrix multiplications at test time (one for





the EEG data, one for each separated audio channel), implying low computational cost.

The CCA-transformed EEG and audio streams are multivariate and produce sets of pairwise correlation coefficients between EEG and audio features. For each pair, the correlation scores are continuously computed within a predefined decoding window (figure 3, green). The duration of the decoding window represents a trade-off between decoding speed and accuracy (Wong *et al* 2018a, de Cheveigné *et al* 2021). In offline studies, we found that our CCA-pipeline can classify attention with an accuracy of around 70%–80% with decoding windows around 6–8 s (see figure 7(C) below for an example of offline decoding accuracies). The windowed correlation component scores are passed to a linear classifier, here

implemented as a two-class support vector machine to decide which of two streams is attended. The choice of classifier is not critical. In the simplest case, the correlation component scores can simply be summed and compared between  $N$  streams.

## 2.4. Audio control

The output of the attention classifier is used to control the gain of the different audio streams in the speech mixture (figure 3 grey). We have explored different audio control strategies. A simple first choice was to map time-varying classifier probabilities to an instantaneous audio gain on each speech stream via a non-linear mapping function. For this, we used a point non-linearity that pulls low classification probabilities towards zero, and high classification probabilities towards a maximum applied gain (see section 3.7 for details). The rationale is to leave the gain unchanged (i.e. no BCI feedback) unless the classifier has reached some level of certainty about the subject's attention.

A drawback of a simple instantaneous coupling between classification scores and gain is the potential of erratic and fast gain changes. Even if infrequent, such acoustic artefacts may be perceived as disturbing by the user. As an alternative strategy, we implemented an attention state space model to control the audio levels (see section 3.8). In this, the rate of gain change varies with the certainty of the classifier. In each classification window, the user's attention state is a function of the previous state and the current information transfer rate estimated from the classifier probabilities. In effect, the state tracker accumulates information over time to estimate the user's current attention state and the relative gains change based on this state. This makes the system less prone to detrimental sudden shifts in gain upon misclassifications while maintaining the possibility of fast state changes when the current information transfer rate of the system is high.

## 3. Methods

In this section we provide more details of the implementation and experimental methods. The busy reader may wish to skip to section 4 for demonstrations of real-time attention steering.

### 3.1. EEG acquisition

In the demonstrations shown in section 4 below, two different EEG acquisition systems were used. For demonstrations of the real-time platform with microphone inputs (section 4.1) we used mBrainTrain's mobile 24-channel SMARTING system (mBrainTrain, Belgrade, Serbia) with a wireless DC amplifier attached to the back of the EEG cap (EasyCap, Hersching, Germany). For experiment I with hearing-impaired users (section 4.2) and experiment II with

audiovisual stimulation (section 4.3), we used a 64-channel Biosemi ActiveTwo system.

### 3.2. EEG training data

For all real-time experiments (sections 4.1–4.3), offline EEG data for training the system were first obtained from each subject. Subjects were presented with two-talker mixtures (audiobooks, one male, one female) presented dichotically for 30–40 mins. The training session was split into 50 s long trials and subjects were instructed to attend to one of the two speakers in each trial. The location of the attended target (attend left vs right) was counterbalanced across trials to avoid spatial bias. In experiment II with audiovisual speech, 10 subjects received additional onscreen visual feedback of the two speakers during training, while 10 other subjects were only presented with the audio. Decoders were trained on the audio envelopes of the speech streams in both cases. In separate experiments, we noted that listening to a single speech stream during training data acquisition resulted in similar closed-loop performance. If this observation can be confirmed, this can simplify the collection of training data for attention decoding experiments considerably (de Cheveigné *et al* 2021). The training data were processed offline with the same processing pipeline as described for the online system below.

### 3.3. Online implementation

The real-time decoder was implemented in Python assembled as processing blocks (see figure 3) using the OpenVibe (1.3.0) graphical BCI software platform for real-time code integration (Renard *et al* 2010). EEG and audio signals were broadcasted to an OpenVIBE acquisition server via labstreaminglayer (Kothe *et al* 2014), a library for networking and routing of time-series data. To synchronize the data streams, trigger pulses generated by an Arduino were sent along both paths (EEG and audio), and a receiver module in OpenVIBE was then used to quantify and compensate for any delay between the streams. i.e. to maintain time-synchronization between data streams.

### 3.4. Online audio processing

To extract audio envelopes in the online system, each separate audio stream was squared, low-pass filtered at 20 Hz (4th order Butterworth), and down-sampled to 64 Hz via decimation. The envelopes were raised to the power of 0.3 to account for the compressive response of the inner ear (Lopez-Poveda *et al* 2003, Fuglsang *et al* 2020). Unlike typical offline studies, this envelope estimation procedure performs an initial low-pass filtering and avoids spectral decomposition in the audio domain for computational efficiency. The envelopes were further passed through a dyadic filterbank implemented as series of low-pass filters followed by a first order differentiator (de

Cheveigné *et al* 2018). The low-pass filtering was performed by convolving the signals with square windows of lengths ranging from 1/32 to 1 s in 10 steps on a logarithmic scale. Differentiation of the low-passed envelopes act as a high-pass filter, effectively creating a filter-bank of bandpass filters in the modulation domain. The audio envelopes were then delayed to account for the difference between stimulus and response by applying a constant shift estimated from the training data. Next, the data were transformed using principal component analysis (PCA) to reduce dimensionality. The number of PCA components retained was determined by cross-validation on the training data, and the PCA transform of the resulting dimensionality was then applied in the online processing. Finally, the multichannel envelopes were multiplied by the CCA weights obtained on the training data.

### 3.5. Online EEG processing

The EEG data were low-pass filtered at 20 Hz (4th order Butterworth) and down-sampled to 64 Hz to match the audio sampling rate. A high-pass filter at 0.1 Hz (2nd order Butterworth) was used to filter out low-frequency drifts, and a common average reference was applied. The data were further filtered to reduce eye-blink activity using a spatial filter obtained using the electroocular channels in the training data (Wong *et al* 2018a). The EEG were passed through a multichannel filtering operation identical to the one applied to the audio envelopes. The data were truncated using PCA, similarly as for the audio data. Finally, the data were transformed using the CCA weights obtained on the training data.

### 3.6. Online audio-EEG classification

The temporally aligned CCA-transformed EEG and audio envelopes were concatenated and the correlation between corresponding CC pairs were computed within a continuously updated decoding window. Decoding windows of 8 s were used in experiment I and windows of 6.5 s were used in experiment II. In both cases, classifications were performed at a rate of 4 Hz, e.g. with a stride of 0.25 s, resulting in an decoding windows with an overlap of 7.75 and 6.25 s, respectively. Each correlation coefficient pair was z-scored based on the training data and input to a linear support vector machine (SVM) classifier with weights obtained on the training data. The classification output was converted to class probabilities for each speech stream being attended based on the training data (Platt *et al* 1999).

### 3.7. Audio gain control

The probability outputs of the classifier was used to control the gain balance between speech streams by attenuating ignored streams in the acoustic feedback to the listener. The baseline level of the speech mixture (without BCI feedback) was set to 60 dB HL,

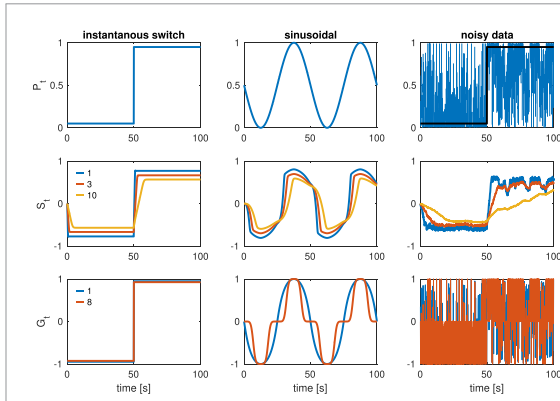


**Figure 4.** Simulations illustrating the behavior of the different audio gain control strategies. Top row: simulated attention classification probabilities  $P_t$ . Middle row: outputs of the state tracker  $S_t$  for different values of the parameter  $K$  in equation (2), i.e. different durations of the decoding window (in secs). Bottom row: outputs of the instantaneous gain control function  $G_t$  for different values of the shape parameter  $k$ . Three different simulations are considered here. The first simulation (left column) assumes an ideal scenario where the classifier correctly identifies an attention switch after 50 s. In the second simulation (middle column) classification probabilities fluctuates sinusoidally. The third simulation (right column) again assumes a target attention switch at 50 s but the classification is noisy. As can be seen, noisy classification results in a fluctuating gain for the instantaneous Weibull mapping function  $G_t$  (bottom) but a smooth gain control for the state tracker (middle).

and BCI feedback could result in a maximum gain difference between speakers of 10 dB. For hearing-impaired listeners, the baseline level was amplified based on their audiometric thresholds to compensate to reduced audibility.

Different gain control functions were investigated. In experiment I, classification probabilities were mapped to a time-varying gain control signal  $G_t$  using a non-linearity corresponding to a modified Weibull cumulative distribution function:

$$G_t = \begin{cases} 1 - e^{-\left(\frac{2P_t-1}{\lambda}\right)^k} & \text{for } P_t \geq 0.5 \\ e^{-\left(\frac{1-2P_t}{\lambda}\right)^k} - 1 & \text{for } P_t < 0.5 \end{cases} \quad (1)$$

where  $P_t$  is the time-varying probability outputs of the classifier. In the current two-talker scenario, speaker A is classified as attended when  $P_t > 0.5$  and speaker B is classified as attended when  $P_t < 0.5$  (and  $P_t = 0.5$  indicates the chance-level likelihood). The parameters  $k$  and  $\lambda$  determines the shape and gain of the Weibull non-linearity (see figure 4). The gain control signal  $G_t$  was scaled to the real-valued interval  $[-1, 1]$  (dividing by  $1 - e^{-(1/\lambda)^k}$ ).  $G_t = -1$  then indicates that full gain should be applied to speaker A while speaker B should be attenuated by the maximum gain difference.  $G_t = 1$  indicates full gain applied to speaker B while speaker A is attenuated. 0 indicates that the system should not attenuate either speaker. The positive and negative values of the gain control signal were each mapped to dB and used to control the audio levels of the two speech streams.

### 3.8. State tracker

In experiment II, the relative gains were controlled via a state tracker. The state tracker implemented a strategy to control the gain based on the state of the attention decoding system. The likelihood probability of the classifier  $P_t$  now controls the *rate* of change in gain. This allows the state to remain stable when the attention classifier yields a chance-level likelihood (i.e. likelihoods toward 0.5), making less prone to detrimental sudden shifts in gain.

The state at time step  $t$  is computed as:

$$S_t = S_{t-1} + C \frac{2}{K \cdot F_s} \text{ITR}_t - \text{sign}(S_{t-1}) |S_{t-1}|^\alpha \quad (2)$$

where  $C$  is the attention state corresponding to the classified speaker:

$$C = \begin{cases} 1 & \text{for } P_t \geq 0.5 \\ -1 & \text{for } P_t < 0.5 \end{cases} \quad (3)$$

with  $P_t$  again being the classifier likelihood.  $\text{ITR}_t$  is the estimated information transfer rate (Wolpaw et al 1998) in bits per classification window of length  $K$  seconds and  $F_s$  is the number of classifications per second, here set to 4 Hz. Using ITR allows the system to adapt its switching speed to the current information rate. In essence, in absence of the  $\text{sign}(S_{t-1}) |S_{t-1}|^\alpha$  term,  $\frac{2}{K \cdot F_s} \text{ITR}$  allows the state to switch from  $-1$  to  $1$  (or vice versa) in one second if the information transfer rate is equivalent to 1 bit/s throughout the entire second. The information transfer rate (in bits per classification window) is computed as:

$$\text{ITR}_t = \log_2(N) + P_t \log_2(P_t) + (1 - P_t) \log_2\left(\frac{1 - P_t}{N - 1}\right) \quad (4)$$

where  $N$  is the number of classes (2 in this case). The exponent  $\alpha$  in equation (2) acts as a hyperparameter that controls the amplitude of state changes and was fixed heuristically at 7.5 in experiment II.

Figure 4 shows simulations that illustrate the behavior of the two different gain control strategies. The top row shows simulated classification probabilities  $P_t$  in three different scenarios (columns). The resulting outputs of the state tracker  $S_t$  and the instantaneous gain function  $G_t$  are shown below in the middle and bottom rows, respectively. The first (leftmost) column simulates an optimally classified instantaneous switch of attention half-way through the trial. The instantaneous gain function (bottom row) shifts the gain accordingly whereas the state tracker (middle row) introduces a delay proportional to the duration of the decoding window. The middle column illustrates how each gain function maps classification probabilities, here simulated as varying sinusoidally. For higher values of  $k$ , the non-linear



mapping in the instantaneous gain function (bottom row) will force the gain to remain unchanged for low classification probabilities and apply maximum gain difference once a certain classification level is reached. The parameter  $k$  controls this non-linearity and its setting allows a trade-off between avoiding gain changes for low probabilities and the overall smoothness of the gain changes. The parameter  $k$  mainly affects the perceptual quality of the gain track and was set heuristically ( $k = 2$ ) in experiment I.

A main motivation for a state space approach to gain control can be illustrated with less-than-optimal classification. A noisy classification of an ideal switch (black) is simulated in the rightmost column in figure 4. In this case, an instantaneous gain control (bottom row) produces a fluctuating gain, whereas the state tracker (middle row) is less prone to these variations. The duration of the decoding window can be increased to make the state tracker less prone to misclassifications but at the expense of slower change in gain upon actual switches in attention. Moreover, the state space model adapts switching time based on the input ITR, i.e. the system can react faster when the current attention classification accuracy is higher. Since the noisy and variable classification scenario is closer to reality for classification based on short EEG segments, we find that a state space approach to gain control like this is generally preferable. In experiment II using the state tracker, we fixed the decoding window to 6.5 s to represent a trade-off between switching speed and random gain fluctuations. The duration of the decoding window could be automatically optimized for performance on training data, but this can result in very long duration windows for poor subjects, effectively making the BCI unresponsive.

### 3.9. Participants

In experiment I with hearing-impaired listeners (section 4.2), 3 young normal-hearing and 3 older hearing-impaired listeners participated. The hearing-impaired subjects participated without their hearing aids on. Instead, a linear frequency-specific amplification was applied based on their audiometric thresholds to restore baseline audibility. In experiment II with audiovisual speech (section 4.3), 20 young normal-hearing listeners participated. Experiments were conducted in accordance with protocol H-16.036.391 approved by the Science Ethics Committee for the Capital region of Denmark.

### 3.10. Closed-loop test procedures

In test sessions with the real-time system, 24 trials (16 closed-loop, 8 open-loop) of 90 s were collected per participant in experiment I (section 4.2), and 36 trials (24 closed-loop, 12 open-loop) of 50 s were collected in experiment II (section 4.3). Pre-recorded two-talker speech audio streams (one male, one female) were fed directly to the real-time decoder in these experiments. Subjects were prompted to attend to one

speaker via an on-screen arrow at the beginning of the trial, and to switch attention to the other speaker halfway through the trial.

### 3.11. Code

A software implementation of the real-time system, including code for the real-time decoding pipeline is available at <https://gitlab.com/cocoha/cocoha-matlab-toolbox>.

## 4. Demonstrations

In this section, we report different real-time experiments performed to demonstrate that the system is functional and usable by a real subject. The demonstrations serve as proof-of-principle use-cases rather than quantitative evaluations of the BCI. First, we show a video demonstration illustrating the system with the WHISPER microphone platform separating speech in a real-world acoustic scenario (section 4.1). Next, we show two experiments to demonstrate attention-steering across subjects with or without hearing impairment (experiment I, section 4.2), and with and without visual input of the speakers face (experiment II, section 4.3). In these experiments, rather than using the microphone platform, we used pre-recorded speech (audiobooks) so that the same speech material could be presented and results compared across different subjects. The real-time system was then used to control the audio gain of the two speech streams.

### 4.1. Demonstration with real talkers

A video illustrating the real-time system is shown below (figure 5). A listener wearing a wireless EEG system focuses attention on either the male or female speaker. The two speakers alternately raise their hands to indicate that the listener should attend to her or him. The WHISPER microphone platform is placed on the table between the talkers and the listener in an ad hoc arrangement. The microphone signals are synchronized on the platform and streamed to the speech separation module that performs online beamforming. The separated speech streams are transmitted to the attention decoding module running on a remote laptop. The decoding module receives and synchronizes EEG and audio streams and performs CCA-based decoding of attention, as described above. The classification output controls the relative gain of the two speech streams in the acoustic feedback presented to the headphones of the subject. The audio track of the left video contains the recorded room audio (the mixed speech). The audio track of the right video contains the beamformed audio presented to the subject, i.e. emulating the hearing aid output. More video demonstrations are available at [cocoha.org/2018/12/31/videos/](https://cocoha.org/2018/12/31/videos/).

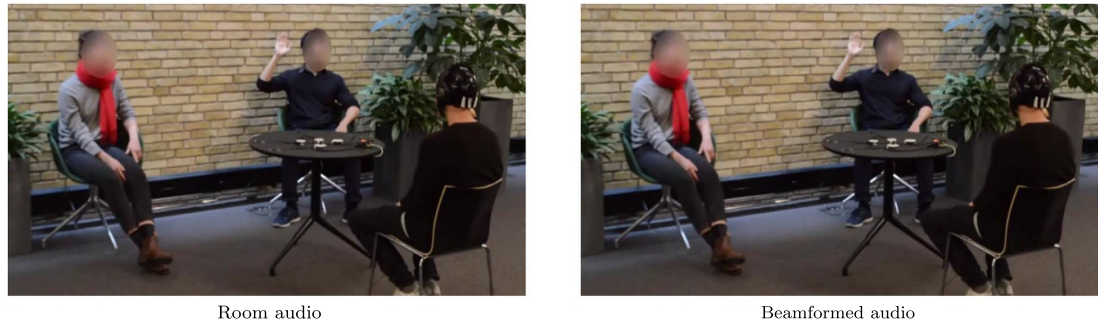


**Figure 5.** Video demonstration of real-time attention decoding. Left: the mixed speech audio recorded in the room. Right: the separated speech audio received by the subject. The subject (facing away from the camera) is wearing a wireless EEG system and headphones receiving the acoustic feedback from the BCI. The two speakers raise their hand alternately to indicate that the listener should attend to them. The WHISPER microphone platform is placed on the table between the listener and the speakers. The videos are available in the [online article](#).

#### 4.2. Experiment I: demonstration with normal-hearing and hearing-impaired listeners

We first tested the real-time system with the clinical target group: older listeners with hearing impairment. Hearing-impaired (HI) listeners with moderate-to-severe hearing loss and normal-hearing (NH) listeners were presented with two competing speech streams in an attention-switching paradigm. To be able to compare results across listeners, pre-recorded speech streams (one male, one female) were presented via loudspeakers to the left and right of the subject. Training data were first obtained with subjects attending one of the two simultaneous speakers on separate 50 s long trials for  $\sim 30$  min (as in offline studies). After training the attention decoder, subjects performed closed-loop steering on 16 test trials, each 90 sec-long. 8 open-loop test trials (without neurofeedback) were collected for comparison. Subjects were prompted to attend to one speaker at the beginning of the trial and to switch attention to the other speaker after 45 s. Online classification was performed in decoding windows of 8 s at a rate of 4 Hz. The classification probabilities were then mapped to an instantaneous gain controlling the balance between the two recorded audio streams (see section 3.7). Maximum classification probability resulted in a maximum gain difference of 10 dB between the two speech streams.

Data from these real-time experiments are shown in figure 6. The average gain applied to the two speech streams as a result of real-time decoding are shown in figure 6(C) and were similar for the HI (blue) and NH (red) listeners. At the onset of trials, the two speakers are presented at the same baseline level (0 dB target-to-masker ratio, TMR). As expected from offline decoding results, the system can correctly classify the attended speaker and the acoustic gain changes accordingly at the onset of the trial. When cued to shift attention, the subject attends to the other speaker. At that point, the target speaker has a negative target-to-masker ratio, here the maximum gain difference of  $-10$  dB TMR (supposing that the system

classified the speaker correctly on the first half of the trial). As can be seen, the gain successfully switches to enhance speaker 2. The average switch time, computed as the duration from the switch cue to the zero-crossing point in the classifier output, was found to be 4.7 s (min = 2.9 s, max = 6.3 s).

#### 4.3. Experiment II: real-time experiment with audiovisual speech

Auditory attention can be decoded while listeners only hear the speaker they are attending, but listeners typically look at the speaker they are listening to in real-world situations. It is unclear whether a BCI trained only on auditory inputs might also work successfully in natural audiovisual conditions. The system could potentially fail to generalize to this mismatching stimulus condition. Alternatively, the visual face may be correlated with audio envelope information (O'Sullivan *et al* 2017a, Pedersen *et al* 2022), and it may be easier to focus auditory attention on a speaker that can be seen, which may in turn improve decoding (O'Sullivan *et al* 2013). Potential visual benefits are important to investigate, for instance in the case where the user wants to switch attention to a previously ignored speaker. In this case, visual information correlated with the speech signal may help 'recover' a target with low audibility.

We tested these questions in a larger experiment. Training data were obtained from normal-hearing participants ( $N = 20$ ) listening to two-talker speech mixtures with or without watching the visual input of the speakers' moving faces (figure 7). The stimuli consisted of two separate pre-recorded speech videos, i.e. the microphone platform was not used in this experiment. During training trials, half of the participants ( $N = 10$ ) received audiovisual stimuli, while the other half ( $N = 10$ ) only received the speech audio. All listeners were then tested using the closed-loop system either with audiovisual stimuli or with the speech audio alone. As a control condition, we included trials without BCI control, i.e. trials

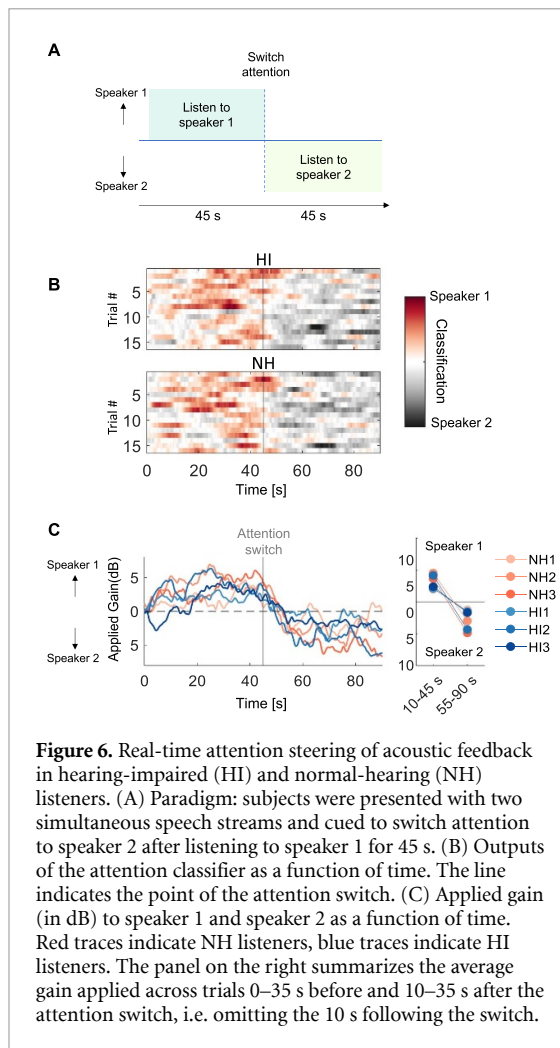


**Figure 6.** Real-time attention steering of acoustic feedback in hearing-impaired (HI) and normal-hearing (NH) listeners. (A) Paradigm: subjects were presented with two simultaneous speech streams and cued to switch attention to speaker 2 after listening to speaker 1 for 45 s. (B) Outputs of the attention classifier as a function of time. The line indicates the point of the attention switch. (C) Applied gain (in dB) to speaker 1 and speaker 2 as a function of time. Red traces indicate NH listeners, blue traces indicate HI listeners. The panel on the right summarizes the average gain applied across trials 0–35 s before and 10–35 s after the attention switch, i.e. omitting the 10 s following the switch.

where the audio gains were left unchanged, referred to as ‘open-loop’ trials. All participants were presented with audiovisual stimuli in the open-loop trials. In test trials of 50 s, subjects were prompted to follow one speaker and then cued to switch attention midway through the trial (i.e. after 25 s), as in experiment I. Rather than the instantaneous gain control function used in experiment I, the audio gains were controlled by a state tracker with a sliding decoding window of 6.5 s and a classification rate of 4 Hz. The rationale of the state tracker is to make the gain less prone to erratic changes in gain with noisy classification outputs (see section 3.7 for a comparison between gain control strategies). The same speech envelope decoding pipeline as described above was used in both audiovisual and audio-only conditions (i.e. no visual features were used in the decoder).

Figure 7 shows data from the real-time experiments with audiovisual speech. Figure 7(B) shows the output of the attention state tracker in the different BCI conditions (closed-loop audio-only, closed-loop audiovisual, open-loop) for the participants trained with audio-only speech (above) and the participants trained with audiovisual speech stimuli (below). Participants were similarly able to steer the BCI with and without seeing the speakers face (CLA vs CLAV),

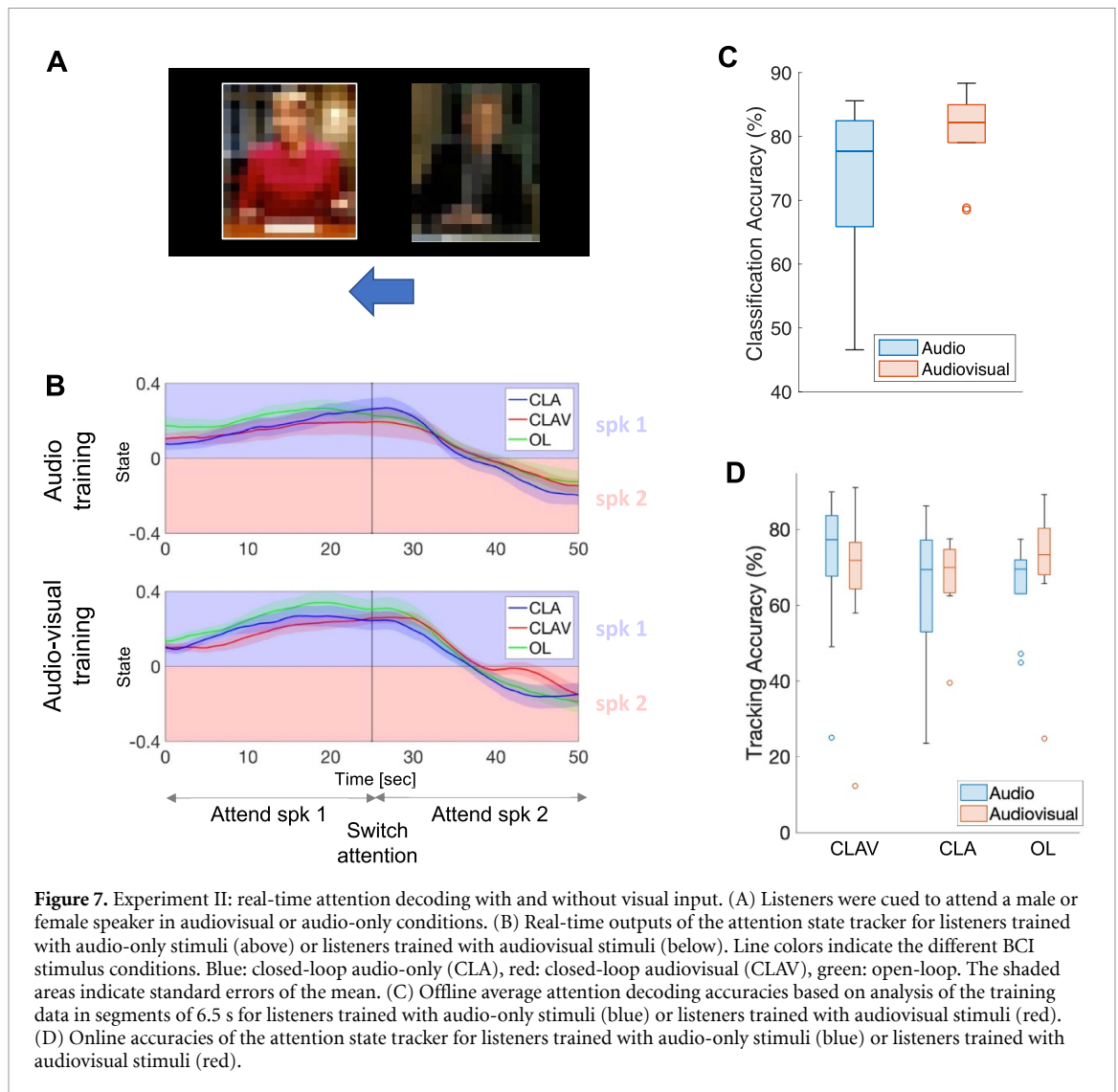
and with and without having seen the speakers face during training. The average switching time of state tracker, again computed as the duration from the switch cue to the zero-crossing point, was found to be 12.6 s, with no difference found between BCI conditions. This slower switching time compared to the ones observed experiment I (section 4.2) indicates that more stable gain variations with the state tracker comes at the expense of a slower reactivity of the BCI. Figure 7(C) shows the attention decoding accuracy obtained with the offline training for participants listening to audio-only speech (blue) and for participants presented with audiovisual speech (red). A modest improvement with visual feedback was seen in the offline training data, but this did not appear to translate to the real-time performance. As a summary measure of BCI tracking performance, figure 7(D) shows the average accuracy of the differential output of the state tracker, i.e. whether the state tracker steps in direction of the target speaker in each classification window. No differences between closed-loop vs open-loop steering were observed, indicating that subjects can switch attention and ‘recover’ an attenuated (previously ignored) speaker. We also did not observe interactions between training modality (audio-only vs audiovisual) and closed-loop modality. It might be expected that participants presented with audiovisual speech during training (red) performed better in the matched audiovisual closed-loop condition, and vice versa for the audio-only group (blue), but this was not observed. While the real-system accurately tracks attention for most subjects, outlier subjects performing at chance-level can be observed (figure 7(D)).

## 5. Discussion

Helping hearing-impaired listeners follow speech in noisy everyday environments remains a fundamental challenge for hearing technologies. In this paper, we provide an overview of a real-time system for acoustic speech separation controlled by attention. As proof-of-principle, we describe initial closed-loop demonstrations indicating that listeners, including elderly people with hearing loss, can steer a gain to enhance the speech sources they are focusing their attention on. If the SNR of speech sources can be directly controlled and improved in this way, a gain in speech understanding follows inherently. Yet, these results should be interpreted with caution. Numerous challenges in bringing such technology to real-life use obviously remain. In the following, we discuss some of the critical prospects and limitations.

### 5.1. Using attention for seamless BCI control

Using attention to steer acoustic feedback has inherent benefits in the context of neural prosthetics. BCIs often require the user to direct attention to the BCI device itself (e.g. as in a ‘P3-speller’ where the subject actively focuses on onscreen letters to spell words).



The attention-controlled hearing instrument, on the other hand, decodes and ‘amplifies’ a natural listening process. Listeners naturally orient attention towards relevant sources in real-world listening situations, allowing them to better perceive relevant sources and suppress background noise. Our BCI assists this natural behavior without interrupting it. If the system correctly decodes attention, then the interaction is seamless. An alternative solution might be to have the user control the speech separation system via an overt device (e.g. selecting which talkers to enhance on a mobile phone). However, such a solution has the detrimental effect that it diverts the user’s attention towards steering the device rather than facilitating it. With the proposed BCI, listeners simply attend to speech as they do in everyday situations to better perceive the relevant source.

### 5.2. BCI based on stimulus-response correlation

A real-time auditory attention decoding system based on stimulus-response correlation is unique in a BCI context. Most existing BCI systems classify brain signals to generate some form of system command (e.g.

steering some application), i.e. the neural data are the only input to the BCI. The BCI discussed here, on the other hand, takes both EEG and audio signals as inputs. Classification now relies on attention-related changes in the *relation* between speech stimulus features and the EEG response. This imposes an important constraint on the classification problem: the BCI can act specifically on the part of the neural response that is related to the stimulus and not on global changes in brain states. This may make the BCI less susceptible to random EEG noise or task-unrelated neural signals.

An alternative solution is to classify a listener’s spatial attention based on changes in EEG alpha power (Kelly *et al* 2005, Geirnaert *et al* 2020, Popov *et al* 2023), i.e. classifying spatial attention based only on EEG features. Yet, this solution suffers from the inherent problem that changes in lateralised EEG alpha power coincide with many task-unrelated changes in the cognitive state of the subject. In pilot studies using this approach, we found that high attention classification accuracies (>90%) could be achieved with short EEG segments (<1 s), but the



system failed to work robustly in closed-loop. A BCI based on stimulus-response metrics may help the critical generalization to real-world conditions beyond those used for training the system.

Other work has investigated neurofeedback based on auditory attention decoding with stimulus-response models. Zink *et al* (2016) provided subjects with visual feedback of online decoding accuracy scores. In a system similar to ours, Aroudi *et al* (2021) used stimulus-response-based attention decoding to steer the relative gain of two speech audio signals. Consistent with our observations reported above, closed-loop decoding accuracy was found to be on par with open-loop decoding (without neurofeedback). This is encouraging, given that closed-loop gain reduction of the ignored speaker could make attention switching more difficult.

Our experiments indicate that it is possible to ‘recover’ previously ignored sources attenuated by up to 10 dB relative to the previous target source, but the boundary conditions for this remain to be explored (Das *et al* 2018). If the stimulus-response relation is not detectable (at very low SNRs), then the BCI cannot classify attention. This may represent a potential weakness of decoding with stimulus-response models. However, offline experiments with audiovisual speech tracking indicate that ‘envelope’ speech tracking may be possible in silent lipreading conditions where the speaker can only be seen (O’Sullivan *et al* 2017a). Visual feedback of the speaker may thus help a BCI track a speech source even when it cannot be heard.

### 5.3. What is accurate decoding?

Attention classification implies a trade-off between speed and accuracy. A critical limitation of the technology is a very low tolerance for misclassification. In our experiments with hearing-impaired listeners (section 4.2), subjective reports from participants indicated that misclassifications were experienced as highly disturbing. With decoding windows below 10 s, the accuracy is currently below 100% correct classification for most subjects. This implies that the system occasionally amplifies the unattended source and suppresses the attended target, which is the opposite of the intended effect. Even if misclassification occurs infrequently (e.g. 10% of time time), the effect may be disastrous. While the BCI is seamless when classification is correct (the subject simply listens to speech), incorrect classification immediately makes the listener aware of the presence of the BCI. In our experiments, some test participants reported that this meant switching strategy to actively steering the device, a process reported as effortful, i.e. the opposite effect of the intended purpose of the BCI. However, in our real-time experiments, such subjective reports were not collected in a systematic manner. Interestingly, Aroudi *et al* (2021) reported subjective ratings of perceived effort but found no effect

of closed-loop steering. Yet, it is not *a priori* clear how decoding accuracy should translate to the subjective perception of BCI control or perceived effort, and examining subjective reports systematically will be important for future closed-loop studies.

As noted in the reported experiments, between-subject variability in real-time decoding accuracy is considerable. Although average performance was relatively high, some participants showed real-time tracking accuracy well below chance level (figure 7(D)). This implies that the BCI effectively works against these subjects (amplifying the speech stream to-be-ignored). The reasons for this behavior are difficult to elucidate. It is possible that some participants become aware of the feedback control and focus on suppressing the speaker to be ignored. It is also possible that occasional amplification of the ignored speaker may cause to the ignored speech to grab the subject’s attention, effectively causing the BCI to get stuck in the wrong state. Identifying such sources of failure in individual users will be critical to the success of such closed-loop technologies.

In the reported experiments, we focus on showing the gain change after the instructed attention switch, but this is arguably a limited metric to capture BCI system performance. A multitude of system design choices can influence BCI performance in ways that are difficult to predict. For instance, different decoding methods or gain control strategies define the ‘reactivity’ of the BCI, which may in turn influence subjects’ attention, influencing decoding performance, etc in a complex loop of events. Non-linear neuro-behavioral feedback systems like this requires dedicated tools of analysis and experimental setups that is beyond the scope of this study.

It is unclear how closed-loop attention steering can best be evaluated in more natural situations while preserving proper experimental control. For simplicity, and for experimental control, we limit ourselves to simple two-talker setup with access to clean audio sources. The same two-talker setup is used to generate data for model training and for closed-loop testing, and it is not clear how performance generalizes beyond this artificial situation, e.g. to different acoustic conditions, different SNRs, different number of speakers, etc.

### 5.4. Better attention decoding?

Improving decoding accuracy may be critical for progress towards a successful technology. Our current implementation relies on linear mappings CCA between audio and EEG features. Non-linear extensions have been proposed in offline attention decoding studies (de Taillez *et al* 2020). An obvious extension is to consider deep learning-based models (Ciccarelli *et al* 2019, Vandecappelle *et al* 2021, Thornton *et al* 2022). However, a number of pitfalls, often deceitfully hidden, should be pointed out. One concern is the limited availability of large amounts of



unbiased training data. In typical attention decoding experiments, listeners are instructed to attend to one speaker in one ear and ignore a different speaker in the other ear. Linear methods based on envelope-EEG correlation can generalize to new speakers because they explicitly model this correlation. However, a non-linear neural network trained to classify attention may simply ignore the EEG and classify acoustic differences between the speakers. To avoid this, experiments that generate training data should be carefully counterbalanced, e.g. attending equally to both speakers, equally attending left/right, etc. Even here, subtle differences may leak into the training data (Rosenblatt *et al* 2024). For instance, speakers may slightly shift voice pitch when speaking over longer durations, and conventional cross-validation procedures (such as leave-one-trial-out) are prone to bias from such details.

### 5.5. What is ground-truth for attention decoding?

Another critical challenge for obtaining high decoding accuracy is the lack of ground truth measures of attention. Decoding models, such as the ones presented here, are trained on data obtained with listeners cued to attend to a given target during training trials. The subjects' attention state is assumed to remain stationary throughout a trial, but the attention state cannot be monitored in any clear way. In everyday tasks, it is difficult to maintain focused attention over time, and attention fluctuates with the internal state of the listener. Attention can also fluctuate with external salient events that occasionally grab attention (Esterman *et al* 2013). When instructed to focus on a speech target in attention decoding experiments, a listener's attention may still occasionally switch to the non-target, or attention may simply drift from the task altogether (Weissman *et al* 2006, Smallwood and Schooler 2015). The lack of measures of such attention dynamics puts decoding models on uncertain ground. An alternative approach may be to dispose of attention labels and focus instead on modelling the stimulus-response relation with simpler stimuli, e.g. listening to a single speaker. For instance, de Cheveigné *et al* (2021) proposed training stimulus-response models based on whether or not a segment of EEG matches the auditory stimulus that evoked it. This approach allows models to be trained in a self-supervised manner. If attention modulates the stimulus-response mapping, then robust stimulus-response models may be key to progress without relying on attention labels.

### 5.6. Need for speed?

Improved decoding accuracies can be obtained by integrating the classification over longer durations, i.e. by sacrificing classification speed. In our experiments, we explored different gain control strategies. Instantaneous gain (used in experiment I) allowed faster average gain changes with attention switches

(<10 s), at the expense of erratic gain changes. Temporal integration with a state space model (in experiment II) stabilized gain fluctuations, but at the expense of slower mean switching times (>10 secs). Similar long switch delays were reported by Aroudi *et al* (2021). In dynamic communication situations involving many talkers, attention may switch rapidly and decoding windows of several seconds are already unfeasible. However, in other situations, longer time constants may be acceptable. In many communication situations, the communication partners remain the same over longer periods—e.g. in a restaurant or at a meeting—where the BCI can slowly 'zoom in' on relevant sources. An alternative decoding strategy may be to identify such long-term stable communication contexts.

### 5.7. Alternative EEG solutions

A critical limitation of the technology is the quality of EEG signals recorded during natural behavior. Cortical signals recorded with scalp EEG are inherently weak and noisy. Our current demonstrations of a real-time BCI are still limited to stationary setups where the listener is sitting still and passively listening. Motion artifacts during natural behavior tend to dramatically surpass the brain signals of interest in scalp EEG. Ear-EEG (EEG recorded in the ear canal or behind the ear) offers feasible solutions for integration with a hearing aid (Looney *et al* 2012, Bleichner and Debener 2017), but does not appear to improve decoding performance (Fiedler *et al* 2017). Invasive cortical recordings improve brain signal SNR considerably, and O'Sullivan *et al* (2017b) demonstrated fast and accurate decoding using electrocorticography (ECoG) recordings in neurological patients (O'Sullivan *et al* 2017b). New multichannel implant solutions are emerging for BCI perspectives (Steinmetz *et al* 2021). Less invasive solutions such as subcutaneous EEG are currently in clinical development (Viana *et al* 2021) and offer interesting perspectives for decoding attention. However, weighing the potential benefits of invasive solutions against the risks for the individual patient is naturally a complex ethical discussion.

### 5.8. Acoustic speech separation solutions

Using a separate speech separation front-end based on distributed microphones was a design choice in our system. Distributed sensors on dedicated hardware offer high-quality speech separation at very low latencies, which is paramount for hearing instrument applications. One drawback of stationary microphones is the need for calibration for a given spatial configuration of sound sources. However, Voice Activity Detectors could be used for dynamic calibration in non-stationary environments. More flexible extensions have recently been proposed, such as 'acoustic swarms' of self-distributing microphones that dynamically locate and separate speech sources

in changing environments (Itani *et al* 2023). Other challenges arise with synchronization of wireless nodes based on radio transmission, which is generally poorly suited for outdoor environments or rooms with plentiful reflective materials like metal surfaces.

An obvious drawback is the need for distributed microphones in the listening space. However, solutions with user-worn microphones (placed on the hearing aid) are also conceivable. Single-channel or two-channel solutions may exploit advances in speech separation within deep learning (Luo and Mesgarani 2018). O'Sullivan *et al* (2017b) already demonstrated that attention can be reliably decoded from the outputs of a single-channel speech separation system, i.e. without assuming access to the clean speech sources (O'Sullivan *et al* 2017b). Successful attention decoding does not follow automatically from previous results with 'clean sources' since some degree of cross-talk between the separated streams must be expected even with high-performing speech separation systems (Ravanelli *et al* 2021, Subakan *et al* 2021).

In our system, the speech separation front-end is separate from the attention decoding process. The task of the decoder is then to decide which of  $N$  separated streams the listener is attending. An alternative framework is to combine the speech separation and decoding steps into one process (Ceolini *et al* 2020a). Since a stimulus-response decoder estimates speech features (typically amplitude envelopes) of the attended stream, these can be used as a 'hint' of the clean audio source. Ceolini *et al* (2020a) presented a neural network-based speech separation system trained on the neural data to extract the clean audio signal directly from the speech mixture. Using ECOG or EEG-reconstructed speech envelopes, the system directly separates the target from the mixture input. Higher envelope reconstruction accuracies were shown to translate into higher separation quality (e.g. an EEG-based reconstruction accuracy of 0.35 corresponds to around 4.2 dB SDR as reported in Ceolini *et al* 2020a). This integrated approach could potentially be expanded to end-to-end neural networks that perform speech separation directly from the raw audio mixture and the continuous EEG (Hosseini *et al* 2021). An advantage of such an approach is that the speech separation system does not have to separate all sources in an acoustic scene (and compare the brain response to each acoustic source) but can focus on separating only the relevant target source from the mixture. This may offer a considerable computational advantage in complex acoustic scenarios with many sources.

### 5.9. Audio control strategy

In our closed-loop experiments, we use the BCI to apply audio gain to the attended and ignored speakers. Successful development of the technology is likely to require development of refined techniques to render the acoustic feedback in ways that are intuitive and comfortable for the user. Re-rendering

the acoustic scene with spatially distributed sources may be critical for real-life usability. It should also be noted that amplification is not the only possible audio control strategy. Hearing aids can, for instance, benefit greatly from selectively applying different dynamic-range compression to the target and background signals (Overby *et al* 2023). Selectively applying fast-acting compression to the attended foreground signal and slow compression to the ignored background avoids the problem of amplifying noise components along with the target speech, a recurrent issue faced by hearing aids today (May *et al* 2020).

### 5.10. Attention training

The BCI is presented here as an assistive technology for the hearing impaired, but other uses can be envisioned. Closed-loop neurofeedback training of attention has been considered as a tool to treat attention deficit disorders, helping patients sustain focus over longer periods (Monastra *et al* 2006, Arns *et al* 2009, Belo *et al* 2021). Closed-loop imaging designs have been proposed in which people monitor their own attention via specially designed visual stimuli that change with attention-driven neurofeedback (Debettencourt *et al* 2015). Our closed-loop system decodes attention during natural listening and modifies the attended speech stimulus itself. This has the advantage of engaging a natural attention process where the 'reward' of successfully attending is inherent in natural behavior (listening becomes easier when attending). Task difficulty can easily be titrated (e.g. via the amount of gain applied) making the system usable in attention training programs. Closed-loop training may also be relevant in context of the proposed hearing technology. It is possible that hearing impaired users may learn to adapt to the closed-loop gain control system, and individual training programs that gradually adjust SNR to improve decoding accuracy over time could be explored.

### 5.11. Looking forward

Going back to the motivations laid out in the Introduction, it is clear that we are now closer to our goal, and yet we remain far from a usable product: the glass is half full, and yet half empty. We successfully assembled and tested a real-time device that covers the full chain from sound waves and brain signals to attention-based selective stimulation at the ear. However, the demonstration remains sketchy at many points. We advanced the state of the art of auditory attention decoding, but latency and accuracy remain below levels required for comfortable use. Progress here may come from better algorithms, better brain signal cues, better understanding of the intentional processes that guide selective auditory attention, or novel brain signal measurement techniques. We designed and assembled a modular distributed microphone array solution to address the problem of delivering high-quality sound to the user.

However, this is just one of a wide range of possible solutions, and latency of wireless communication remained a problem. Further progress in this part of the design space depends crucially on low-latency protocols for wireless communication, and much work remains to evaluate this approach relative to others. Our experiments with human subjects, including typical potential users, indicate that the concept is workable but limited by current performance levels. These experiments also point to the need of a more complete methodology for future studies. Overall, these outcomes demonstrate that the goal is worth pursuing, and the software that we provide may help future endeavors in that direction. This work should be seen as an early milestone along the road towards a cognitively controlled hearing aid.

### Data availability statement

Code implementing the real-time decoding system is available at <https://gitlab.com/cocoha/cocoha-matlab-toolbox>.

### Acknowledgment

This work was supported by the EU H2020-ICT Grant 644732 (COCOHA), and Grants ANR-10-LABX-0087 IEC and ANR-10-IDEX-0001-02 PSL. It draws on work performed at the 2016 Telluride Neuromorphic Engineering workshop, and benefitted from the boundless enthusiasm of Shihab Shamma, Nima Mesgarani, Daniel Pressnitzer, Tobi Delbruck, and others. Alain de Cheveigné is funded in part by the FrontCog Grant ANR-17-EURE-0017. Søren A Fuglsang is funded in part by the Grant NNF17OC0027872 from the Novo Nordisk Foundation. Søren A Fuglsang, Jonatan Mårcher-Rørsted, and Jens Hjortkjær are funded in part by the Center for Auditory Neuroscience supported by the William Demant Foundation.

### ORCID iDs

Jens Hjortkjær  <https://orcid.org/0000-0003-3724-3332>

Daniel D E Wong  <https://orcid.org/0000-0002-7781-1149>

Alessandro Catania  <https://orcid.org/0009-0009-6415-3384>

Enea Ceolini  <https://orcid.org/0000-0002-2676-0804>

Søren A Fuglsang  <https://orcid.org/0000-0001-8111-8665>

Ilya Kiselev  <https://orcid.org/0000-0002-5055-4314>

Giovanni Di Liberto  <https://orcid.org/0000-0002-7361-0980>

Shih-Chii Liu  <https://orcid.org/0000-0002-7557-045X>

Torsten Dau  <https://orcid.org/0000-0001-8110-4343>

Malcolm Slaney  <https://orcid.org/0000-0001-9733-4864>

Alain de Cheveigné  <https://orcid.org/0000-0002-7305-1891>

### References

- Akram S, Presacco A, Simon J Z, Shamma S A and Babadi B 2016 Robust decoding of selective auditory attention from meg in a competing-speaker environment via state-space modeling *NeuroImage* **124** 906–17
- Arns M, De Ridder S, Strehl U, Breteler M and Coenen A 2009 Efficacy of neurofeedback treatment in ADHD: the effects on inattention, impulsivity and hyperactivity: a meta-analysis *Clin. EEG Neurosci.* **40** 180–9
- Aroudi A, Fischer E, Serman M, Puder H and Doclo S 2021 Closed-loop cognitive-driven gain control of competing sounds using auditory attention decoding *Algorithms* **14** 287
- Aroudi A, Mirkovic B, De Vos M and Doclo S 2016 Auditory attention decoding with EEG recordings using noisy acoustic reference signals *2016 IEEE Int. Conf. on Acoustics, Speech and Signal Processing (ICASSP)* (IEEE) pp 694–8
- Aroudi A, Mirkovic B, De Vos M and Doclo S 2019 Impact of different acoustic components on EEG-based auditory attention decoding in noisy and reverberant conditions *IEEE Trans. Neural Syst. Rehabil. Eng.* **27** 652–63
- Belo J, Clerc M and Schön D 2021 EEG-based auditory attention detection and its possible future applications for passive BCI *Front. Comput. Sci.* **3** 661178
- Bleichner M G and Debener S 2017 Concealed, unobtrusive ear-centered EEG acquisition: cEEgrids for transparent EEG *Front. Hum. Neurosci.* **11** 163
- Bronkhorst A W 2000 The cocktail party phenomenon: a review of research on speech intelligibility in multiple-talker conditions *Acta Acust. united Acust.* **86** 117–28 (<https://www.ingentaconnect.com/content/dav/aaua/2000/00000086/00000001/art00016>)
- Ceolini E, Hjortkjær J, Wong D D, O'Sullivan J, Raghavan V S, Herrero J, Mehta A D, Liu S-C and Mesgarani N 2020a Brain-informed speech separation (BISS) for enhancement of target speaker in multitalker speech perception *NeuroImage* **223** 117282
- Ceolini E, Kiselev I and Liu S-C 2020b Evaluating multi-channel multi-device speech separation algorithms in the wild: a hardware-software solution *IEEE/ACM Trans. Audio Speech Lang. Process.* **28** 1428–39
- Ceolini E and Liu S-C 2019 Combining deep neural networks and beamforming for real-time multi-channel speech enhancement using a wireless acoustic sensor network *2019 IEEE 29th Int. Workshop on Machine Learning for Signal Processing (MLSP)* (IEEE) pp 1–6
- Cherry E C 1953 Some experiments on the recognition of speech, with one and with two ears *J. Acoust. Soc. Am.* **25** 975–9
- Ciccharelli G, Nolan M, Perricone J, Calamia P T, Haro S, O'Sullivan J, Mesgarani N, Quatieri T F and Smalt C J 2019 Comparison of two-talker attention decoding from EEG with nonlinear neural networks and linear methods *Sci. Rep.* **9** 1–10
- Das N, Bertrand A and Francart T 2018 EEG-based auditory attention detection: boundary conditions for background noise and speaker positions *J. Neural Eng.* **15** 066017
- Dau T, Kollmeier B and Kohlrausch A 1997 Modeling auditory processing of amplitude modulation. I. Detection and masking with narrow-band carriers *J. Acoust. Soc. Am.* **102** 2892–905
- Dau T, Roersted J M, Fuglsang S and Hjortkjær J 2018 Towards cognitive control of hearing instruments using EEG measures of selective attention *J. Acoust. Soc. Am.* **143** 1744–1744

- de Cheveigné A, Slaney M, Fuglsang S A and Hjortkjaer J 2021 Auditory stimulus-response modeling with a match-mismatch task *J. Neural Eng.* **18** 046040
- de Cheveigné A, Wong D D E, Di Liberto G M, Hjortkjaer J, Slaney M and Lalor E 2018 Decoding the auditory brain with canonical component analysis *NeuroImage* **172** 206–16
- de Taillez T, Kollmeier B and Meyer B T 2020 Machine learning for decoding listeners' attention from electroencephalography evoked by continuous speech *Eur. J. Neurosci.* **51** 1234–41
- Debettencourt M T, Cohen J D, Lee R F, Norman K A and Turk-Browne N B 2015 Closed-loop training of attention with real-time brain imaging *Nat. Neurosci.* **18** 470–5
- Ding N and Simon J Z 2012a Emergence of neural encoding of auditory objects while listening to competing speakers *Proc. Natl Acad. Sci.* **109** 11854–9
- Ding N and Simon J Z 2012b Neural coding of continuous speech in auditory cortex during monaural and dichotic listening *J. Neurophysiol.* **107** 78–89
- Esterman M, Noonan S K, Rosenberg M and DeGutis J 2013 In the zone or zoning out? tracking behavioral and neural fluctuations during sustained attention *Cereb. Cortex* **23** 2712–23
- Fiedler L, Wöstmann M, Graversen C, Brandmeyer A, Lunner T and Obleser J 2017 Single-channel in-ear-EEG detects the focus of auditory attention to concurrent tone streams and mixed speech *J. Neural Eng.* **14** 036020
- Fuglsang S A, Dau T and Hjortkjaer J 2017 Noise-robust cortical tracking of attended speech in real-world acoustic scenes *Neuroimage* **156** 435–44
- Fuglsang S A, Märcher-Rørsted J, Dau T and Hjortkjaer J 2020 Effects of sensorineural hearing loss on cortical synchronization to competing speech during selective attention *J. Neurosci.* **40** 2562–72
- Geirnaert S, Francart T and Bertrand A 2020 Fast EEG-based decoding of the directional focus of auditory attention using common spatial patterns *IEEE Trans. Biomed. Eng.* **68** 1557–68
- Geirnaert S, Vandecappelle S, Alickovic E, de Cheveigne A, Lalor E, Meyer B T, Miran S, Francart T and Bertrand A 2021 Electroencephalography-based auditory attention decoding: toward neurosteered hearing devices *IEEE Signal Process. Mag.* **38** 89–102
- Golumbic E M Z et al 2013 Mechanisms underlying selective neuronal tracking of attended speech at a “cocktail party” *Neuron* **77** 980–91
- Ha J, Baek S-C, Lim Y and Chung J H 2023 Validation of cost-efficient EEG experimental setup for neural tracking in an auditory attention task *Sci. Rep.* **13** 22682
- Hosseini M, Celotti L and Plourde E 2021 Speaker-Independent Brain Enhanced Speech Denoising ICASSP 2021 - 2021 IEEE Int. Conf. on Acoustics, Speech and Signal Processing (ICASSP) (06–11 June 2021, Toronto, ON, Canada) pp 1310–4
- Itani M, Chen T, Yoshioka T and Gollakota S 2023 Creating speech zones with self-distributing acoustic swarms *Nat. Commun.* **14** 5684
- Kelly S, Lalor E, Reilly R and Foxe J 2005 Independent brain computer interface control using visual spatial attention-dependent modulations of parieto-occipital alpha *Conf. Proc. 2nd Int. IEEE EMBS Conf. on Neural Engineering* (IEEE) pp 667–70
- Kiselev I, Ceolini E, Wong D, De Cheveigne A and Liu S-C 2017 Whisper: wirelessly synchronized distributed audio sensor platform 2017 IEEE 42nd Conf. on Local Computer Networks Workshops (LCN Workshops) (IEEE) pp 35–43
- Kochkin S 2010 Marketrak VIII: consumer satisfaction with hearing aids is slowly increasing *Hear. J.* **63** 19–20
- Kothe C, Medine D, Boulay C, Grivich M and Stenner T 2014 Lab streaming layer (LSL)
- Lesica N A 2018 Why do hearing aids fail to restore normal auditory perception? *Trends Neurosci.* **41** 174–85
- Looney D, Kidmose P, Park C, Ungstrup M, Rank M L, Rosenkranz K and Mandic D P 2012 The in-the-ear recording concept: user-centered and wearable brain monitoring *IEEE Pulse* **3** 32–42
- Lopez-Poveda E A, Plack C J and Meddis R 2003 Cochlear nonlinearity between 500 and 8000 hz in listeners with normal hearing *J. Acoust. Soc. Am.* **113** 951–60
- Luo Y and Mesgarani N 2018 Tasnet: time-domain audio separation network for real-time, single-channel speech separation 2018 IEEE Int. Conf. on Acoustics, Speech and Signal Processing (ICASSP) (IEEE) pp 696–700
- May T, Kowalewski B and Dau T 2020 Scene-aware dynamic-range compression in hearing aids *The Technology of Binaural Understanding* (Springer) pp 763–99
- Mesgarani N and Chang E F 2012 Selective cortical representation of attended speaker in multi-talker speech perception *Nature* **485** 233–6
- Miran S, Akram S, Sheikhattar A, Simon J Z, Zhang T and Babadi B 2018 Real-time tracking of selective auditory attention from m/EEG: a Bayesian filtering approach *Front. Neurosci.* **12** 262
- Mirkovic B, Debener S, Jaeger M and De Vos M 2015 Decoding the attended speech stream with multi-channel EEG: implications for online, daily-life applications *J. Neural Eng.* **12** 046007
- Monastera V J, Lynn S, Linden M, Lubar J F, Gruzelić J and La Vaque T J 2006 Electroencephalographic biofeedback in the treatment of attention-deficit/hyperactivity disorder *J. Neurother.* **9** 5–34
- O'Sullivan A E, Crosse M J, Di Liberto G M and Lalor E C 2017a Visual cortical entrainment to motion and categorical speech features during silent lipreading *Front. Hum. Neurosci.* **10** 679
- O'Sullivan J A, Crosse M J, Power A J and Lalor E C 2013 The effects of attention and visual input on the representation of natural speech in EEG 2013 35th Annual Int. Conf. of the IEEE Engineering in Medicine and Biology Society (EMBC) (IEEE) pp 2800–3
- O'Sullivan J A, Power A J, Mesgarani N, Rajaram S, Foxe J J, Shinn-Cunningham B G, Slaney M, Shamma S A and Lalor E C 2015 Attentional selection in a cocktail party environment can be decoded from single-trial EEG *Cerebr. Cortex* **25** 1697–706
- O'Sullivan J, Chen Z, Herrero J, McKhann G M, Sheth S A, Mehta A D and Mesgarani N 2017b Neural decoding of attentional selection in multi-speaker environments without access to clean sources *J. Neural Eng.* **14** 056001
- Overby N, Dau T and May T 2023 A data-driven distance metric for evaluating the effects of dynamic range compression in adverse conditions *Trends Hear.* **27** 23312165231192302
- Pedersen N F, Dau T, Hansen L K and Hjortkjaer J 2022 Modulation transfer functions for audiovisual speech *PLOS Comput. Biol.* **18** e1010273
- Platt J et al 1999 Probabilistic outputs for support vector machines and comparisons to regularized likelihood methods *Adv. Large Margin Classifiers* **10** 61–74
- Popov T, Gips B, Weisz N and Jensen O 2023 Brain areas associated with visual spatial attention display topographic organization during auditory spatial attention *Cerebr. Cortex* **33** 3478–89
- Power A J, Foxe J J, Forde E-J, Reilly R B and Lalor E C 2012 At what time is the cocktail party? a late locus of selective attention to natural speech *Eur. J. Neurosci.* **35** 1497–503
- Ravanelli M et al 2021 Speechbrain: a general-purpose speech toolkit (arXiv:2106.04624)
- Renard Y, Lotte F, Gibert G, Congedo M, Maby E, Delannoy V, Bertrand O and Lécuyer A 2010 Openvibe: an open-source software platform to design, test and use brain-computer interfaces in real and virtual environments *Presence* **19** 35–53
- Rosenblatt M, Tejavibulya L, Jiang R, Noble S and Scheinost D 2024 Data leakage inflates prediction performance in



- connectome-based machine learning models *Nat. Commun.* **15** 1829
- Slaney M, Lyon R F, Garcia R, Kemler B, Gnegy C, Wilson K, Kanevsky D, Savla S and Cerf V G 2020 Auditory measures for the next billion users *Ear Hear.* **41** 131S–139S
- Smallwood J and Schooler J W 2015 The science of mind wandering: empirically navigating the stream of consciousness *Annu. Rev. Psychol.* **66** 487–518
- Steinmetz N A et al 2021 Neuropixels 2.0: a miniaturized high-density probe for stable, long-term brain recordings *Science* **372** eabf4588
- Subakan C, Ravanelli M, Cornell S, Bronzi M and Zhong J 2021 Attention is all you need in speech separation *ICASSP 2021-2021 IEEE Int. Conf. on Acoustics, Speech and Signal Processing (ICASSP)* (IEEE) pp 21–25
- Thakkar K, Hai J and Elhilali M 2024 Investigating self-supervised deep representations for EEG-based auditory attention decoding *ICASSP 2024-2024 IEEE Int. Conf. on Acoustics, Speech and Signal Processing (ICASSP)* (IEEE) pp 1241–5
- Thornton M, Mandic D and Reichenbach T 2022 Robust decoding of the speech envelope from EEG recordings through deep neural networks *J. Neural Eng.* **19** 046007
- Van Eyndhoven S, Francart T and Bertrand A 2016 EEG-informed attended speaker extraction from recorded speech mixtures with application in neuro-steered hearing prostheses *IEEE Trans. Biomed. Eng.* **64** 1045–56
- Vandecappelle S, Deckers L, Das N, Ansari A H, Bertrand A and Francart T 2021 EEG-based detection of the locus of auditory attention with convolutional neural networks *Elife* **10** e56481
- Viana P F, Duun-Henriksen J, Glasstetter M, Dümpelmann M, Nurse E S, Martins I P, Dumanis S B, Schulze-Bonhage A, Freestone D R and Brinkmann B H et al 2021 230 days of ultra long-term subcutaneous EEG: seizure cycle analysis and comparison to patient diary *Ann. Clin. Trans. Neurol.* **8** 288–93
- Weissman D H, Roberts K, Visscher K and Woldorff M 2006 The neural bases of momentary lapses in attention *Nat. Neurosci.* **9** 971–8
- Wolpaw J R, Ramoser H, McFarland D J and Pfurtscheller G 1998 EEG-based communication: improved accuracy by response verification *IEEE Trans. Rehabil. Eng.* **6** 326–33
- Wong D D E et al 2018b A closed-loop platform for real-time attention control of simultaneous sound streams *ARO 41st Annual Midwinter Meeting (Abstract)*
- Wong D D, Fuglsang S A, Hjortkjær J, Ceolini E, Slaney M and De Cheveigne A 2018a A comparison of regularization methods in forward and backward models for auditory attention decoding *Front. Neurosci.* **12** 531
- Yost W A 1997 The cocktail party problem: Forty years later *Binaural and Spatial Hearing in Real and Virtual Environments*, ed R H Gilkey and T R Anderson (Lawrence Erlbaum) pp 329–47
- Zink R, Baptist A, Bertrand A, Van Huffel S and De Vos M 2016 Online detection of auditory attention in a neurofeedback application *Proc. 8th Int. Workshop on Biosignal Interpretation* pp 1–4